

The structure and fluxionality of $[\text{Fe}_3(\text{CO})_{10}(\text{dppe})]$; a merry-go-round with no sense of direction

Harry Adams, Sylvana C.M. Agostinho¹, Brian E. Mann*, Stephen Smith

Department of Chemistry, The University of Sheffield, Sheffield, S3 7HF, UK

Received 3 March 2000; accepted 16 May 2000

Dedicated to Professor Martin Bennett on the occasion of his 65th birthday.

Abstract

The crystal structure of $[\text{Fe}_3(\text{CO})_{10}(\text{dppe})]$ has been determined. The $\text{Ph}_2\text{PCH}_2\text{CH}_2\text{PPh}_2$ ligand bridges the $\text{Fe}(\mu\text{-CO})_2\text{Fe}$ edge and is markedly non-planar. The non-planarity inverts with $\Delta G_{211}^\ddagger = 48.4 \pm 0.5 \text{ kJ mol}^{-1}$. The carbonyls on the bridged iron atoms exchange with the axial ones by the merry-go-round mechanism with $\Delta G_{195}^\ddagger = 43.4 \pm 0.5 \text{ kJ mol}^{-1}$. Despite the non-planar dppe ligand producing a chiral molecule, the merry-go-round exchange goes with equal rate in both directions. This is the first example of a six-toothed failed ratchet. © 2000 Elsevier Science S.A. All rights reserved.

Keywords: Fluxionality; Iron clusters; Carbonyl phosphines

1. Introduction

For a number of years, we have been investigating the mechanisms of fluxionality of $[\text{Fe}_3(\text{CO})_{12}]$ and its derivatives. At very low temperature, the concerted bridge-opening bridge-closing mechanism continues to be fast with a $\Delta G^\ddagger < 20 \text{ kJ mol}^{-1}$, unless the dynamic pathway is blocked by ligand substitution, see Scheme 1 [1].

The lowest energy dynamic pathway that can be studied using NMR spectroscopy is the merry-go-round mechanism, which generally has a $\Delta G^\ddagger \sim 40 \text{ kJ mol}^{-1}$, and can be stopped on the NMR timescale at -100°C , see Scheme 2.

At higher temperatures, a variety of exchange mechanisms come into play. In general, these mechanisms are reasonably defined, but there is a problem at the unbridged iron atom. For example in $[\text{Fe}_3(\text{CO})_{11}\{\text{P}(\text{OMe})_3\}]$, at -101°C , three ^{13}CO signals are observed with an intensity ratio 5:5:1 [2]. On warming

above -100°C , the two signals of intensity 5 exchange, presumably due to the merry-go-round mechanism, with $\Delta G^\ddagger = 37 \text{ kJ mol}^{-1}$. At higher temperature, the unique carbonyl exchanges with the other ten carbonyls with $\Delta G^\ddagger = 62.7 \text{ kcal mol}^{-1}$. The mechanism of this highest energy process is not known, but has normally been attributed to the trigonal twist mechanism centred on the unbridged iron atom [2]. In 1996, it was reported that for $[\text{Fe}_3(\text{CO})_{10}(\text{dppe})]$, exchange at the unbridged iron atom does not occur at room temperature putting the activation energy in excess of 67 kJ mol^{-1} [3]. It therefore appeared that it was worth looking at this compound again.

When this compound was examined, the investigation changed from a routine check of a literature report to a study of a new type of failed ratchet. In 1997, Kelly et al., dared to ask if it was possible to build molecular ratchets [4]. They examined a potential molecular ratchet based on triptycene and asked if the presence of a chiral centre caused a group to rotate preferentially in one direction. At first sight this question appeared to be sensible, but it breaks the predictions of the second law of thermodynamics, and Feynman has explained why molecular ratchets will not work [5]. The attempt of Kelly et al. failed as theory would predict, as did a more elaborate attempt by

* Corresponding author.

E-mail address: b.mann@sheffield.ac.uk (B.E. Mann).

¹ Permanent address: Instituto de Química de São Carlos, Universidade de São Paulo, Cx Postal 780, CEP 13.560-970. São Carlos, São Paulo, Brazil.

Espinet et al. [6]. Both these examples involve the rotation of a three-toothed ‘ratchet’ against a chiral centre. Recently, Kelly et al. have partially succeeded in driving rotation in one direction, but this required chemical reactions as the energy source [7]. Koumura et al. have used light as the energy source to produce a mono-directional rotor [8]. In the case of $[\text{Fe}_3(\text{CO})_{10}(\text{dppe})]$ there are six carbonyls rotating relative to a chiral centre, increasing the number of ‘teeth’ in the ratchet from three to six, but with no energy source.

2. The crystal structure of $[\text{Fe}_3(\text{CO})_{10}(\text{dppe})]$

The molecular structure is shown in Fig. 1. There are two independent molecules of $[\text{Fe}_3(\text{CO})_{10}(\text{dppe})]$ and one molecule of solvent, CH_2Cl_2 , in the unit cell. Selected bond lengths and bond angles are given in Table 1. The structures are very similar and only one molecule is shown in Fig. 1. In both molecules, the dppe ligand is coordinated to the two iron atoms on the $\text{Fe}(\mu\text{-CO})_2\text{Fe}$ edge of the Fe_3 triangle.

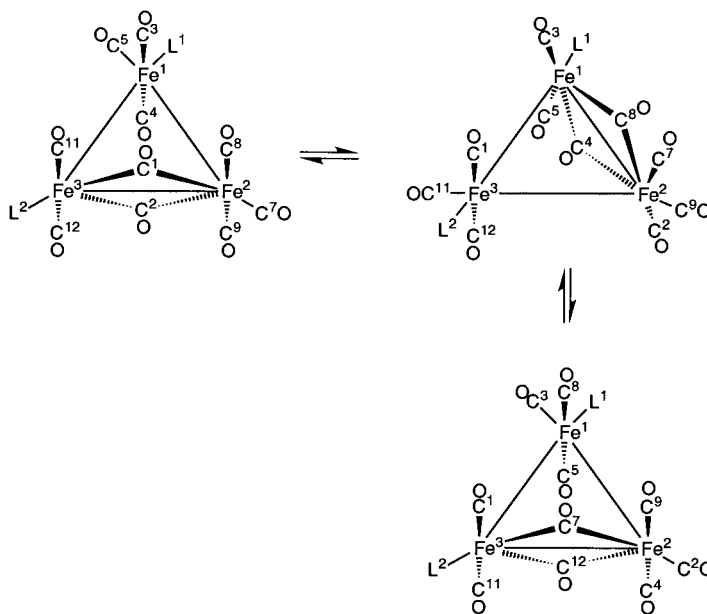
In both molecules, the $\text{Ph}_2\text{PCH}_2\text{CH}_2\text{PPh}_2$ adopts a conformation where there is a marked zig-zag arrangement of the $\text{P-CH}_2\text{-CH}_2\text{-P}$ atoms. see Fig. 2. As a result, the molecule is chiral.

The bridging carbonyls are asymmetric with significantly different Fe-C distances, being more so in molecule 1 than in molecule 2. This is a common distortion in derivatives of $[\text{Fe}_3(\text{CO})_{12}]$ and is an indication that the molecules are distorting according to the concerted bridge-opening bridge-closing dynamic

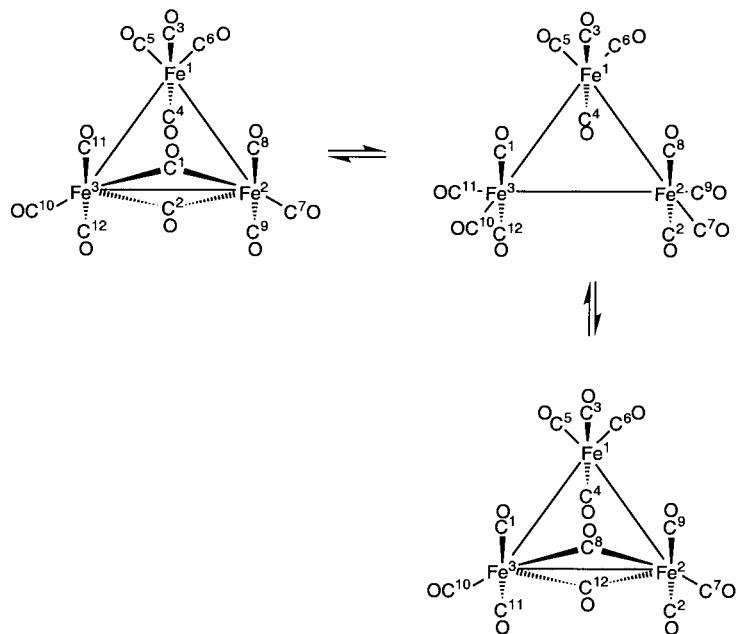
pathway [1]. In both molecules, one of the phosphorus atoms remains approximately in the plane of the Fe_3 triangle defining the S_{10} axis for the concerted bridge-opening bridge-closing mechanism and the ligands rotate about this axis. This is illustrated in Fig. 3 for molecule 2, where the rotation is most marked.

3. Variable temperature NMR investigation of $[\text{Fe}_3(\text{CO})_{10}(\text{dppe})]$

The presence of a phosphorus ligand off the S_{10} axis of the icosahedron of ligands prevents the concerted bridge-opening bridge-closing mechanism operating, leaving only the merry-go-round mechanism, which is frozen out at -92°C . At this temperature the low temperature $^{13}\text{C-NMR}$ spectrum is consistent with the pseudo C_2 symmetry of the crystal structure. The zig-zag conformation of the $\text{P-CH}_2\text{-CH}_2\text{-P}$ group results in the loss of a plane of symmetry through the molecule. As a result there are two sets of phenyl signals due to Ph^1, Ph^4 and Ph^2, Ph^3 , see (1). Similarly, the axial carbonyls on Fe^2 and Fe^3 are inequivalent with two sets of signals due to $\text{C}^8\text{O}, \text{C}^{12}\text{O}$ and $\text{C}^9\text{O}, \text{C}^{11}\text{O}$. As a result, the $^{13}\text{C-NMR}$ spectrum of $[\text{Fe}_3(\text{CO})_{10}(\text{dppe})]$ at -92°C in CD_2Cl_2 shows five ^{13}CO signals in the ratio 2:2:2:2:2 at δ 244.3, 217.9, 216.7, $^2J(^{31}\text{P}^{13}\text{C}) = 12$ Hz, 213.8, $^2J(^{31}\text{P}^{13}\text{C}) = 7$ Hz, and 207.7, two phenyl signals at δ 135.6, {ipso, $^1J(^{31}\text{P}^{13}\text{C}) = 46$ Hz}, 130.9, {ipso, $^1J(^{31}\text{P}^{13}\text{C}) = 43$ Hz, partially obscured}, δ 133.495, (*ortho*, $^2J(^{31}\text{P}^{13}\text{C}) = 10$ Hz), δ 129.7 (*ortho*, $^2J(^{31}\text{P}^{13}\text{C})$



Scheme 1. The concerted bridge-opening bridge-closing mechanism for $[\text{Fe}_3(\text{CO})_{10}\text{L}^1\text{L}^2]$. This causes carbonyls $\text{C}^1\text{O}, \text{C}^{11}\text{O}, \text{C}^{12}\text{O}, \text{C}^2\text{O}$ and C^7O to circulate around the $\text{Fe}^2\text{-Fe}^3$ edge of the Fe_3 triangle and carbonyls $\text{C}^3\text{O}, \text{C}^5\text{O}, \text{C}^4\text{O}, \text{C}^9\text{O}$ and C^8O to concertedly circulate around the $\text{Fe}^1\text{-Fe}^2$ edge. When $\text{L}^1 = \text{L}^2 = \text{CO}$, the $\text{Fe}^1\text{-Fe}^2$ and $\text{Fe}^1\text{-Fe}^3$ edges are equivalent and the circulation can occur around any pair of edges.



Scheme 2. The merry-go-round mechanism applied to $[\text{Fe}_3(\text{CO})_{12}]$. This causes carbonyls C^1O , C^{11}O , C^{12}O , C^2O , C^9O and C^8O to circulate around the Fe^2 – Fe^3 edge of the Fe_3 triangle. A similar circulation around other edges causes all the carbonyls to exchange.

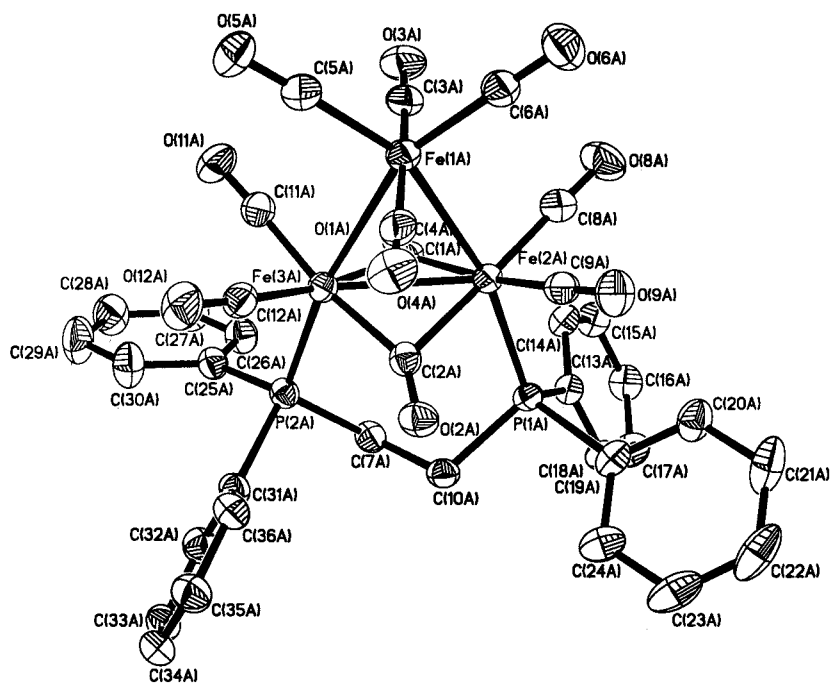


Fig. 1. The structure of $[\text{Fe}_3(\text{CO})_{10}(\text{dppe})]$. The hydrogen atoms are omitted.

= 9 Hz), δ 128.2 (*meta*, $^3J(^{31}\text{P}^{13}\text{C}) = 10$ Hz), δ 128.0 (*meta*, $^3J(^{31}\text{P}^{13}\text{C}) = 10$ Hz), δ 130.7 (*para*), and δ 129.5 (*para*), and 22.1, $\{\text{CH}_2$, doublet, $N(^{31}\text{P}^{13}\text{C}) = 26$ Hz $\}$. It is relatively unusual for the puckering of a $\text{Ph}_2\text{PCH}_2\text{CH}_2\text{PPh}_2$ to be sufficient to produce the inequivalence of groups on the NMR time scale. This effect of puckering has been noted previously for

$[\text{Ir}_4(\text{CO})_{10}(\text{dppe})]$, making the two phosphorus atoms inequivalent at low temperature [9].

At -78°C , the merry-go-round mechanism becomes noticeable, with the carbonyl signals at δ 244.3, 216.7 and 213.8 broadening equally. This permits these carbonyls to be assigned to the bridging carbonyls C^1O and C^2O at 244.3, and the two pairs of axial carbonyls,

Table 1
Selected bond lengths and bond angles for the two independent molecules of $[\text{Fe}_3(\text{CO})_{10}(\text{dppe})]$

Molecule 1		Molecule 2	
Bond	(Å)	Bond	(Å)
Fe(1)–Fe(2)	2.6945(6)	Fe(1A)–Fe(3A)	2.6894(6)
Fe(1)–Fe(3)	2.7073(6)	Fe(1A)–Fe(2A)	2.7108(6)
Fe(2)–C(2)	1.863(3)	Fe(2A)–C(1A)	1.895(3)
Fe(2)–C(1)	2.190(3)	Fe(2A)–C(2A)	2.067(3)
Fe(2)–P(1)	2.2251(8)	Fe(2A)–P(1A)	2.2426(8)
Fe(2)–Fe(3)	2.5437(6)	Fe(2A)–Fe(3A)	2.5407(6)
Fe(3)–C(1)	1.869(3)	Fe(3A)–C(2A)	1.899(3)
Fe(3)–C(2)	2.193(3)	Fe(3A)–C(1A)	2.104(3)
Fe(3)–P(2)	2.2388(8)	Fe(3A)–P(2A)	2.2284(8)
Angle	(°)	Angle	(°)
C(9)–Fe(2) –Fe(3)	45.75(8)	C(9A)–Fe(2A) –Fe(3A)	54.29(8)
C(10)–Fe(2) –Fe(3)	57.23(9)	C(10A)–Fe(2A) –Fe(3A)	47.32(7)
P(1)–Fe(2) –Fe(3)	106.44(2)	P(1A)–Fe(2A) –Fe(3A)	106.50(2)
C(9)–Fe(3) –Fe(2)	57.08(10)	C(9A)–Fe(3A) –Fe(2A)	47.00(7)
C(10)–Fe(3) –Fe(2)	45.58(7)	C(10A)–Fe(3A) –Fe(2A)	53.14(8)
P(2)–Fe(3) –Fe(2)	107.34(2)	P(2A)–Fe(3A) –Fe(2A)	107.32(2)
Fe(3)–C(9) –Fe(2)	77.17(11)	Fe(2A)–C(9A) –Fe(3A)	78.71(10)
Fe(2)–C(10) –Fe(3)	77.19(11)	Fe(3A)–C(10A) –Fe(2A)	79.54(10)
Fe(2)–Fe(1) –Fe(3)	56.184(14)	Fe(3A)–Fe(1A) –Fe(2A)	56.130(15)
Fe(3)–Fe(2) –Fe(1)	62.162(16)	Fe(3A)–Fe(2A) –Fe(1A)	61.510(14)
Fe(2)–Fe(3) –Fe(1)	61.654(17)	Fe(2A)–Fe(3A) –Fe(1A)	62.360(14)

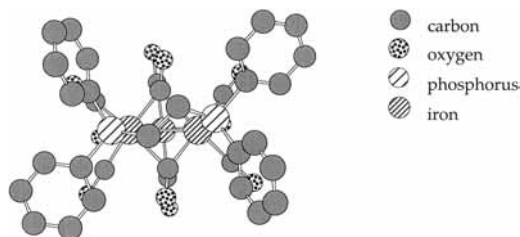


Fig. 2. A projection of molecule 2, with the iron atoms aligned horizontally, with the unbridged iron atom going into the plane of the paper. The hydrogen atoms are omitted. Note the zig-zag arrangement of the $\text{Ph}_2\text{PCH}_2\text{CH}_2\text{PPh}_2$ group.

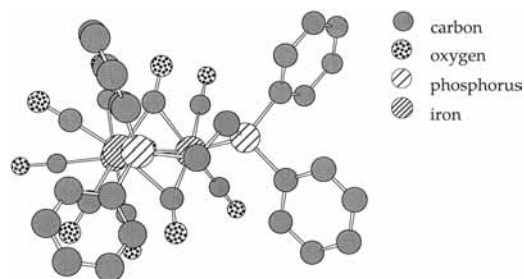


Fig. 3. A projection through P^2 and C^6 of molecule 1 to illustrate the rotation of the ligands around the S_{10} axis. The hydrogen atoms are omitted. Note that P^2 lies close to the plane of the Fe_3 triangle and P^1 and the carbonyls lying off the S_{10} axis going through P^2 and C^6 have rotated around the S_{10} axis.

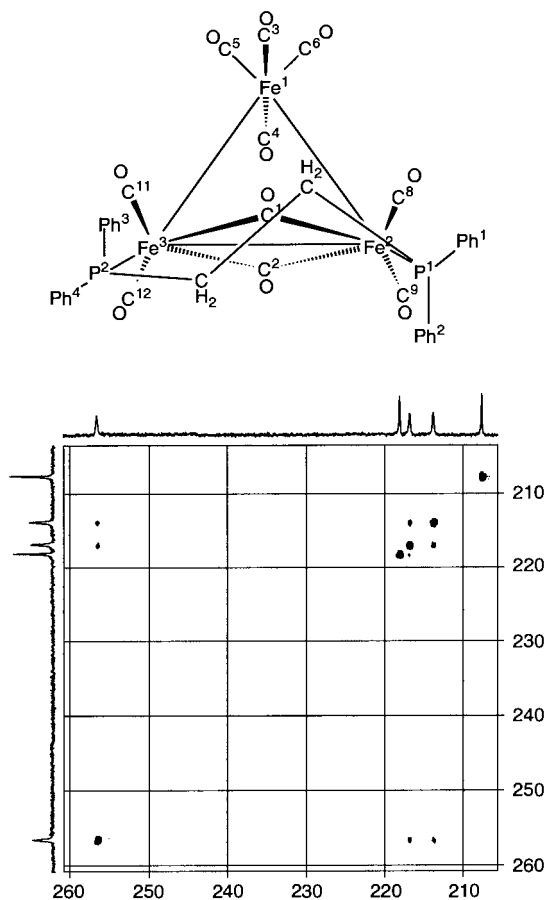


Fig. 4. A diagonalized 100.62 MHz ^{13}C EXSY NMR spectrum of the carbonyls of $[\text{Fe}_3(\text{CO})_{10}(\text{dppe})]$ in CD_2Cl_2 at -78°C , showing the exchange between C^1O , C^2O , C^8O , C^{12}O and C^9O , C^{11}O . The spectrum was acquired using an exchange delay of 0.02 s in $4\text{k} \times 256$ data points and a sweep width of 16 129 Hz.

C^8O , C^{12}O and C^9O , C^{11}O , at δ 216.7 and 213.8, although the relative assignments of these terminal carbonyls are unknown. This leaves C^3O and C^4O at δ 217.9 and C^5O and C^6O at δ 207.7. The exchange was checked using EXSY, see Fig. 4. As required for this assignment for the ‘merry-go-round’ mechanism there is

exchange between each site with an exchange rate of 9.5 s^{-1} , and $\Delta G_{195}^{\ddagger} = 43.4 \pm 0.5 \text{ kJ mol}^{-1}$ [10].

The arrangement of groups in $[\text{Fe}_3(\text{CO})_{10}(\text{dppe})]$ approximates to a ratchet, with the phenyl groups acting as pawls into the rotating carbonyl ‘teeth’ and the pucker of the dppe ligand provides the chiral centre. Hence the compound is potentially another molecular ratchet, but has a six-toothed ring in contrast to the three-toothed ring of the compounds previously studied [5,7]. No evidence was found for preferential exchange in either direction. The cross peak in the EXSY spectrum without diagonalization between C^1O , C^2O and C^8O , C^{12}O is identical to that between C^1O , C^2O and C^9O , C^{11}O , see Fig. 5. This shows that the rate of exchange from C^1O , C^2O to C^8O , C^{12}O is identical to that from C^1O , C^2O to C^9O , C^{11}O . Hence there is no preferred direction for the rotation of the merry-go-round. This is consistent with the failure of earlier

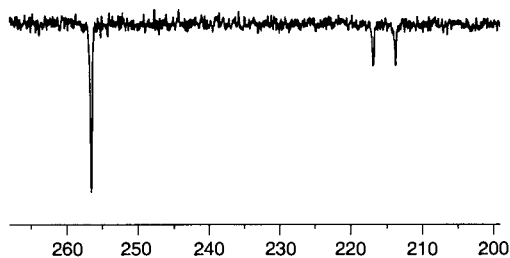


Fig. 5. A horizontal cross section through the EXSY spectrum shown in Fig. 4 before diagonalization, showing the exchange from C^1O , C^2O to C^8O , C^{12}O and C^9O , C^{11}O .

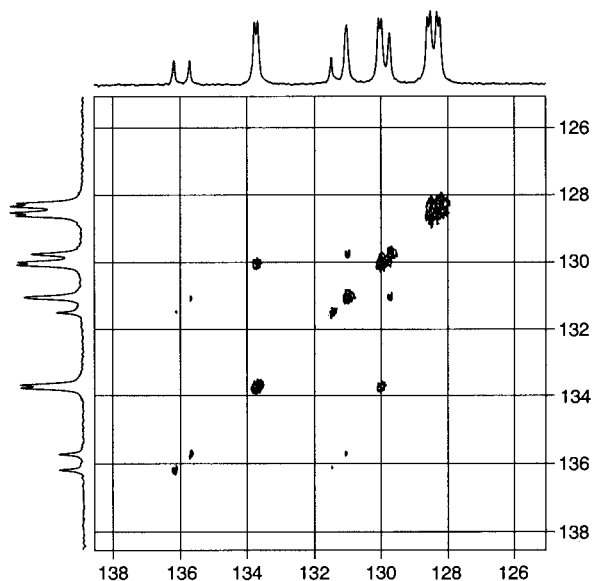


Fig. 6. A diagonalized 100.62 MHz ^{13}C EXSY NMR spectrum of the phenyl signals of $[\text{Fe}_3(\text{CO})_{10}(\text{dppe})]$ in CD_2Cl_2 at -62°C , showing the exchange between C^1O , C^2O , C^8O , C^{12}O and C^9O , C^{11}O . The spectrum was acquired using an exchange delay of 0.05 s in $1\text{k} \times 256$ data points and a sweep width of 1358.7 Hz.

attempts to find molecular ratchets [5,7] and the predictions of Feynman [6].

Although the dppe fails to select the direction of rotation of the ‘merry-go-round’, it does appear to act as a brake, raising the activation energy from $\Delta G^{\ddagger} = 37$ to 41 kJ mol^{-1} in $[\text{Fe}_3(\text{CO})_{12-n}\{\text{P}(\text{OMe})_3\}_n]$ ($n = 1-3$) compounds to $43.4 \pm 0.5 \text{ kJ mol}^{-1}$ in $[\text{Fe}_3(\text{CO})_{10}(\text{dppe})]$. It is not certain that the dppe acts as a brake. The change is relatively small and could arise from the dppe ligand being a better σ -donor ligand than $\text{P}(\text{OMe})_3$, thus enhancing the stability of the bridging structure or could be as a result of the phenyl groups obstructing the path of the merry-go-round.

At -62°C , the exchange of the phenyl groups becomes noticeable, with the phenyl signals broadening equally. The exchange was checked using EXSY, see Fig. 6. The data were only analysed for the *ortho* carbon signals because of overlap of signals and the long T_1 for the *ipso* carbon signals. The analysis gave an exchange rate of 4.5 s^{-1} , and $\Delta G_{211}^{\ddagger} = 48.4 \pm 0.5 \text{ kJ mol}^{-1}$ for the ring inversion. Clearly this is substantially larger than the activation energy for the merry-go-round and is not coupled to it.

At 20°C , the ^{13}C -NMR spectrum shows a broad averaged signal for the six carbonyls undergoing the merry-go-round fluxionality. The axial and equatorial carbonyls on the unbridged iron are clearly resolved as sharp signals at δ 219.54 and 208.22. Usually exchange of the carbonyls at the unbridged iron occurs at room temperature resulting in a broad signal. In the case of $[\text{Fe}_3(\text{CO})_{11}\{\text{P}(\text{OMe})_3\}]$ this exchange occurs with a $\Delta G^{\ddagger} = 62.7 \text{ kJ mol}^{-1}$. This raises the possibility that the exchange of the unique carbonyl with the remaining ten carbonyls, observed in $[\text{Fe}_3(\text{CO})_{11}\{\text{P}(\text{OMe})_3\}]$, is not due to the trigonal twist mechanism as previously suggested [2]. If it was, then the same dynamic process would be expected to have a similar activation energy in $[\text{Fe}_3(\text{CO})_{10}(\text{dppe})]$. It is possible that an alternative mechanism such as one involving a phosphorus ligand going into the axial position is necessary to provide the pathway for exchange. In the case of $[\text{Fe}_3(\text{CO})_{10}(\text{dppe})]$, such a pathway could be blocked by the presence of the chelate ring.

4. Experimental

Crystal data for $\text{C}_{37}\text{H}_{26}\text{Cl}_2\text{Fe}_3\text{O}_{10}\text{P}_2$; $M = 930.97$, crystallises from dichloromethane as black blocks; crystal dimensions $0.30 \times 0.20 \times 0.20 \text{ mm}$. Monoclinic, $a = 20.382(3)$, $b = 12.3037(17)$, $c = 31.109(4) \text{ \AA}$, $\beta = 94.718(3)^\circ$ $U = 7774.9(19) \text{ \AA}^3$, $Z = 8$, $D_{\text{calc}} = 1.591 \text{ Mg m}^{-3}$, space group $P2_1/n$ (a non-standard setting of $P2_1/c C_2h$ No. 14), $\text{Mo-K}\alpha$ radiation ($\lambda = 0.71073 \text{ \AA}$), $\mu(\text{Mo-K}\alpha) = 1.380 \text{ mm}^{-1}$, $F(000) = 3760$, see Table 2.

Table 2
Crystal data and structure refinement for $[\text{Fe}_3(\text{CO})_{10}(\text{dppe})]$

Identification code	$[\text{Fe}_3(\text{CO})_{10}(\text{dppe})]$
Empirical formula	$\text{C}_{37}\text{H}_{26}\text{Cl}_2\text{Fe}_3\text{O}_{10}\text{P}_2$
Formula weight	930.97
Temperature (K)	150(2)
Wavelength (Å)	0.71073
Crystal system	Monoclinic
Space group	$P2_1/n$
Unit cell dimensions	
a (Å)	20.382(3)
b (Å)	12.3037(17)
c (Å)	31.109(4)
α (°)	90
β (°)	94.718(3)
γ (°)	90
Volume (Å ³)	7774.9(19)
Z	8
D_{calc} (Mg m ⁻³)	1.591
Absorption coefficient (mm ⁻¹)	1.380
$F(000)$	3760
Crystal size (mm ³)	0.30 × 0.20 × 0.20
Theta range for data collection (°)	1.15–28.43
Index ranges	$-27 \leq h \leq 21$, $-16 \leq k \leq 16$, $-30 \leq l \leq 41$
Reflections collected	50 143
Independent reflections	18 536 [$R_{\text{int}} = 0.0386$]
Completeness to $\theta = 28.43^\circ$	94.6%
Absorption correction	Semi-empirical
Max. and min. transmission	0.7698 and 0.6822
Refinement method	Full-matrix least-squares on F^2
Data/restraints/parameters	18536/0/973
Goodness-of-fit on F^2	1.002
Final R indices [$I > 2\sigma(I)$]	$R_1 = 0.0420$, $wR_2 = 0.1052$
R indices (all data)	$R_1 = 0.0626$, $wR_2 = 0.1192$
Largest difference peak and hole (e Å ⁻³)	1.143 and -0.899

Data collected were measured on a Bruker Smart CCD area detector with Oxford Cryosystems low temperature system. Cell parameters were refined from the setting angles of 48 reflections (θ range $1.15 < 28.43^\circ$),

Reflections were measured from a hemisphere of data collected of frames each covering 0.3 degrees in omega. Of the 50 143 reflections measured, all of which were corrected for Lorentz and polarisation effects and for absorption by semi-empirical methods based on symmetry-equivalent and repeated reflections (minimum and maximum transmission coefficients 0.6822 and 0.7698) 13 649 independent reflections exceeded the significance level $|F|/\sigma(|F|) > 4.0$. The structure was solved by direct methods and refined by full-matrix least-squares methods on F^2 . Hydrogen atoms were placed geometrically and refined with a riding model (including torsional freedom for methyl groups) and with U_{iso} constrained to be 1.2 (1.5 for methyl groups) times U_{eq} of the carrier atom. Refinement converged at a final $R = 0.0420$ ($wR_2 = 0.1192$, for all 18 536 data,

973 parameters, mean and maximum δ/σ 0.000, 0.001) with allowance for the thermal anisotropy of all non-hydrogen atoms. Minimum and maximum final electron density -0.899 and 1.143 e \AA^{-3} .

A weighting scheme $w = 1/[\sigma^2(F_o^2) + (0.0729 * P)^2 + 0.00 * P]$ where $P = (F_o^2 + 2 * F_c^2)/3$ was used in the latter stages of refinement. Complex scattering factors were taken from the program package SHELXTL [11] as implemented on the Viglen Pentium computer.

The NMR spectra were recorded on a Bruker AMX400 NMR spectrometer in CD_2Cl_2 . The EXSY spectra were recorded using a relaxation delay of 2 s, and the Bruker phase sensitive two-dimensional program with TPPI, noesytp, which has been modified to include composite pulse decoupling.

$[\text{Fe}(\text{CO})_5]$, dppe, $\text{Me}_3\text{NO} \cdot 2\text{H}_2\text{O}$, and CD_2Cl_2 were purchased from Aldrich. $[\text{Fe}_3(\text{CO})_{12}]$ was synthesised according to the literature [12]. $\text{Me}_3\text{NO} \cdot 2\text{H}_2\text{O}$ was dried by azeotropic distillation using toluene and Dean–Stark distillation equipment. The synthesis and characterisation of $[\text{Fe}_3(\text{CO})_{10}(\text{dppe})]$ has been described previously [3].

5. Supplementary material

The crystal structure has been deposited at the Cambridge Crystallographic Data Centre and allocated the deposition number CCDC 141939. Copies of this information may be obtained free of charge from The Director, CCDC, 12 Union Road, Cambridge CB2 1EZ, UK (Fax: +44-1223336033; e-mail: deposit@ccdc.cam.ac.uk or www: <http://www.ccdc.cam.ac.uk>)

Acknowledgements

We wish to thank the Instituto de Química de São Carlos-USP, FAPESP, Brazil, and the University of Sheffield for financial support.

References

- [1] B.E. Mann, J. Chem. Soc. Dalton Trans. (1997) 1457.
- [2] H. Adams, N.A. Bailey, G.W. Bentley, B.E. Mann, J. Chem. Soc. Dalton Trans. (1989) 1831.
- [3] E. Stein, F.Y. Fujiwara, J. Organomet. Chem. 525 (1996) 31.
- [4] (a) T.R. Kelly, I. Tellitu, J.P. Sestelo, Angew. Chem. Int. Ed. 36 (1997) 1866. (b) T.R. Kelly, J.P. Sestelo, I. Tellitu, J. Org. Chem. 63 (1998) 3655.
- [5] R.P. Feynman, R.B. Leighton, M. Sands, The Feynman Lectures on Physics, vol. 1, Addison-Wesley, Reading, MA, 1963, (Chapter 46).
- [6] M.A. Alonso, J.A. Casares, P. Espinet, K. Soulantica, Angew. Chem. Int. Ed. 38 (1999) 533.

- [7] T.R. Kelly, H. De Silva, R.A. Silva, *Nature* 401 (1999) 150.
- [8] N. Koumura, R.W.J. Zijlstra, R.A. van Delden, N. Harada, B.L. Feringa, *Nature* 401 (1999) 152.
- [9] R. Ros, A. Scrivanti, V. Albano, D. Braga, L. Garlaschelli, *J. Chem. Soc. Dalton Trans.* (1986) 2411.
- [10] The rate of exchange was determined using D2DNMR, E.W. Abel, T.P.J. Coston, K.G. Orrell, V. Šik, D.J. Stephenson, *J. Magn. Reson.* 70 (1986) 34.
- [11] SHELXL version. An integrated system for solving and refining crystal structures from diffraction data (Revision 5.1), Bruker AXS Ltd.
- [12] W. McFarlane, G. Wilkinson, *Inorg. Synth.* 8 (1966) 181.